Applied Mathematics and Computation 377 (2020) 125150

Contents lists available at ScienceDirect

Applied Mathematics and Computation

journal homepage: www.elsevier.com/locate/amc

Graph-theoretical derivation of brain structural connectivity☆

G. Giacopelli[a,b], M. Migliore[b,1], D. Tegolo[a,b,1,*]

[a] Department of Mathematics and Informatics, University of Palermo, Palermo, Italy
[b] Institute of Biophysics, National Research Council, Palermo, Italy

ARTICLE INFO

Article history:
Received 20 September 2019
Revised 29 January 2020
Accepted 9 February 2020
Available online 3 March 2020

Keywords:
Connectome
Neuronal networks
Random graphs

ABSTRACT

Brain connectivity at the single neuron level can provide fundamental insights into how information is integrated and propagated within and between brain regions. However, it is almost impossible to adequately study this problem experimentally and, despite intense efforts in the field, no mathematical description has been obtained so far. Here, we present a mathematical framework based on a graph-theoretical approach that, starting from experimental data obtained from a few small subsets of neurons, can quantitatively explain and predict the corresponding full network properties. This model also changes the paradigm with which large-scale model networks can be built, from using probabilistic/empiric connections or limited data, to a process that can algorithmically generate neuronal networks connected as in the real system.

1. Introduction

The brain is a complex organ composed by neurons, fundamental units of this system; their connectivity has a crucial role in determining the dynamics of both individual neurons and the whole network. The system can be considered a directed graph with the neurons soma as nodes and synaptic connections among neurons as edges. The computational properties of different neurons and subnetworks depend on their topological organization [1–3], and numerous brain disorders can be associated with abnormal topological structure [4,5]. Although several important results on the computational properties of neurons can be investigated at the single cell level, e.g. to explain some chaotic behaviors [6], or to suggest an empirical explanation for the storage capacity of an individual neuron [7,39], discovering the general rules underlying the connectivity properties of their networks is a fundamental step to figure out how information is integrated and propagated within and between brain regions.

The need to find a rule explaining how brain cells are connected cannot be overemphasized. Any large initiative on brain research dedicates quite significant efforts to this problem. Since it would have an enormous influence on our understanding of how the brain works. It is well known that several electrophysiological properties of neurons and networks can be modeled as a system of ordinary nonlinear differential equations, so it may be questioned why investigate brain networks

☆ This work has been supported by the EU Horizon 2020 Framework Programme for Research and Innovation under the Specific Grant Agreement 785907 (Human Brain Project SGA2).

* Corresponding author at:
E-mail addresses: giuseppe.giacopelli@unipa.it (G. Giacopelli), michele.migliore@cnr.it (M. Migliore), domenico.tegolo@unipa.it (D. Tegolo).

[1] These authors contributed equally.

https://doi.org/10.1016/j.amc.2020.125150

with graph theory. The rationale is that graph theory has been proven to be of a great help in understanding network properties and operations. Infection models such as the Susceptible Infected (-Recovered) (SI (R)) [8], are typical examples. In these cases, a model that takes adequately into account the heterogeneity of the degrees observed in various real networks represents the underlying network topology. Furthermore, Aledo et al. in [9] highlight a network of attractors in which the graphs allow a better understanding of the system dynamics.

Since the central nervous system can be considered a complex network consisting of a large number of mutually interacting excitatory and inhibitory neurons, it is appropriate to define a mathematical model capable of representing the distribution of a large neuronal network [10–14]. Herculano-Houzel et al. estimated that the central nervous system network involves more than 86 billion neurons [15], this implies fourfold synaptic connections and an enormous equivalent processing per second. Therefore, understanding neuronal distributions and their relative functioning is a challenge that has fascinated researchers in recent decades.

The different scientific areas of mathematics appear among those that can give insightful contributions for a better understanding of the neuronal distribution and related interconnections. Theoretical and applicative advances in the area of graph theory provide a convenient framework for the study of brain structural connectivity, a problem that has not been solved so far. In humans, the current state of the art relies on experimental data of macroscopic connectivity obtained from diffusion tractography [16], but its resolution and the problems with its validation makes it practically impossible to investigate the single cell connectome [17]. Anatomical tracers in non-human studies (reviewed in [18]) give more information, but they are still based on specialized labeling methods that also have shortcomings [19]. Therefore, it should be clear that discovering the general rules underlying the connectivity properties of brain cells is a fundamental step to figure out how information is integrated and propagated within and between brain regions.

Here we suggest an innovative model, exploiting the properties of exponential and power-law models. We were able to use the available, but necessarily sparse, experimental data to generalize the rules underlying brain connectivity. This will provide the basis for a better interpretation of experimental data, for analyzing in more details how the brain processes information and, ultimately, to build large-scale model networks reproducing the observed connectivity. The model is tested against detailed experimental and large-scale modeling data on the hippocampus and neocortex.

2. Materials and methods

2.1. Principles of graph theory

We start by defining:

1. a graph as an entity $G = (V, E)$ composed by a number of nodes $N_G = V(G)$,
2. a set of edges $E(G) \subset V(G) \times V(G)$,
3. $D_G(i)$ as the number of the edges, where i is the node number (also called a vertex),
4. an adjacency matrix $A = (a_{ij})$ as

$$a_{ij} = \begin{cases} 1, & \text{if } (i,j) \in E(G) \\ 0, & \text{if } (i,j) \notin E(G) \end{cases}$$

In this paper we will consider only directed graphs. In a directed graph the vertex have independent incoming and outgoing connections. The adjacency matrix is thus asymmetrical, and we need to distinguish between the in- and out-degree of a vertex i, i.e. the number of incoming and outgoing edges respectively. We will denote them as $D^I_G(i)$ and $D^O_G(i)$, respectively.

2.2. Exponential and power law models

In order to illustrate how our algorithm is implemented, consider the two well-known classes of random graphs, called exponential (introduced in [20]) and power law (described in [21]). In an exponential model, the probability that exist an edge starting from node i and arriving at node j is exactly p, a constant, for any distinct i and j and the in- and out-degree distribution are

$$P\left(D^I_G = k\right) = P\left(D^O_G = k\right) = p^k (1-p)^{N-1-k} \binom{N-1}{k}.$$

The model is called exponential because the tail of the functions describing the indegree and outdegree decays faster than any power law. In power law networks, called BA models (from Barabasi and Albert, who first described them in [22]), the underlying assumption is the existence of a preferential connection between nodes, and the probability for a node to have k connections decreases as $k^{-\gamma}$. The construction of a power law model is based on an integer positive random variable Σ, with distribution σ_k, and expected value c ($c = \mathbb{E}(\sigma_k)$). As previously demonstrated [21], for degrees k much greater than an arbitrary constant a, the indegree distribution can be approximated by

$$p^I_k = \frac{B\left(k+a, 2+\frac{a}{c}\right)}{B\left(a, 1+\frac{a}{c}\right)} \approx k^{-\left(2+\frac{a}{c}\right)},$$

where $B(x, y)$ is the Beta function [23]. The outdegree will follow a Σ distribution with a spike at 0,

$$P(D^O_{PR} = k) = \left(\frac{m_0}{N}\delta_0(k) + \frac{N - m_0}{N}\sigma_k\right),$$

where $\delta_0(k)$ is the discrete Dirac's delta distribution, and m_0 is a free parameter, calculated with a function described in [21].

For the indegree of this model, a particularly important case is when $a = c$,

$$p^I_k = \frac{B(k + a, 3)}{B(a, 2)} = \frac{2(a + 1)a}{(a + k + 2)(a + k + 1)(a + k)} \approx k^{-3},$$

for k much higher than a. The value of -3 is the typical tail value assumed for a scale free model.

3. Theory: Our model

3.1. Initial considerations

Networks rarely exhibit an exponential tail in their distributions, and biological networks often exhibit a tail behavior that can be approximated by a power law [24–28]. The tails behavior is a very important property, because it gives a direct estimation of the network hubs (which are correlated to the way in which information can propagate in the brain [29]). However, the tail alone it is not sufficient to completely describe the properties of a network, since the entire range of connectivity should be considered. The major problem is that neither the exponential or power models can represent the full range of connectivity exhibited by biological networks [24–28]. With respect to a biological network, exponential models have too few highly connected nodes, and power law models have too many nodes with low connectivity. This situation is schematically illustrated in Fig. 1, where we plot a typical example of indegree distribution for an exponential model (Fig. 1, red curve), a power law model (see Fig. 1, blue curve), and a stereotypical case of a brain network [27,28]. As can be seen, an exponential model can reproduce the low-connectivity range of a biological network and a power law model can fit the tail, i.e. the high-connectivity range. This is the reason why, in most cases, the common choice to analyze experimental findings is to ignore the low connectivity range and fit only the tail of the distributions with a power low model, as schematically shown in the inset of Fig. 1 (purple tail fitting line). In this work, instead, we propose a mathematical model based on a convolutional approach in which a power law and exponential model are convolved to obtain a distribution exhibiting the same properties observed experimentally for the entire range of connectivity.

To explain how these models are convolved, we start from u_k and v_k, two probability distributions.

Definition 1. We define the convolution distribution as

$$[u_q * v_q]_k = \sum_{q=-\infty}^{+\infty} u_q v_{k-q}$$

in particular if u_k and v_k are zero for negative values of k, then it holds

$$[u_q * v_q]_k = \sum_{q=0}^{k} u_q v_{k-q}.$$

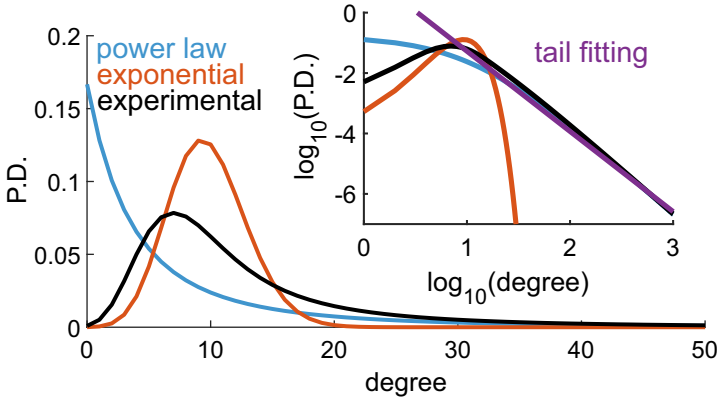

Fig. 1. Degree distribution for different type of networks. Typical Probability Density (PD) distribution of degrees for a power law model, an exponential model, and a biological network [30]. The inset shows the LogLog representation of the three models, and a line fitting the tail of the power law model.

Theorem 1. *Let's consider two directed graphs F and G with N_F and N_G nodes, with indegree distributions f_k^I and g_k^I and outdegree distributions f_k^O and g_k^O. Let's create the directed graph TM starting from the disjoint union of F and G. We will then define p_{FG} and p_{GF} in [0,1] as the probability that a node of F is connected to a node of G and the probability that a node of G is connected to a node of F, respectively.*

The degree distributions of the TM graph are:

$$P(D_{TM}^I = k) = \left[f_q^I * \left(\frac{N_F}{N_F+N_G} B_{p_{GF}}^{N_G}(q) + \frac{N_G}{N_F+N_G} B_{p_{FG}}^{N_F}(q) \right) \right]_k,$$

$$P(D_{TM}^O = k) = \left[f_q^O * \left(\frac{N_F}{N_F+N_G} B_{p_{FG}}^{N_G}(q) + \frac{N_G}{N_F+N_G} B_{p_{GF}}^{N_F}(q) \right) \right]_k.$$

Proof of Theorem 1. Let's start observing that

$$\begin{aligned} P(D_{TM}^I = k) &= P((D_{TM}^I = k) \cap (V \in F)) + P((D_{TM}^I = k) \cap (V \in G)) \\ &= P(D_{TM}^I = k | V \in F) P(V \in F) + P(D_{TM}^I = k | V \in G) P(V \in G) \\ &= P(D_{TM}^I = k | V \in F) \frac{N_F}{N_F+N_G} + P(D_{TM}^I = k | V \in G) \frac{N_G}{N_F+N_G}, \end{aligned}$$

briefly

$$P(D_{TM}^I = k) = P(D_{TM}^I = k | V \in F) \frac{N_F}{N_F+N_G} + P(D_{TM}^I = k | V \in G) \frac{N_G}{N_F+N_G}. \tag{1}$$

We now introduce the notation $P(D_{TM}^I = k | V \in F) = P((D_{TM}^I | V \in F) = k)$, where the random variable $(D_{TM}^I | V \in F)$ is the sum of two random variables $(D_{TM}^I | V \in F) = (D_F^I | V \in F) + (D_G^I | V \in F)$. The first term represents the degree contribution of the graph *F* in the degree of a node of *F*. The second term is the contribution of *G*.

So we can write

$$P(D_{TM}^I = k | V \in F) = P\Big(\big((D_F^I | V \in F) + (D_G^I | V \in F) \big) = k \Big).$$

Now we observe that

$$\Big(\big((D_F^I | V \in F) + (D_G^I | V \in F) \big) = k \Big) = \bigcup_{q=-\infty}^{+\infty} \Big(\big((D_F^I | V \in F) = q \big) \cap \big((D_G^I | V \in F) = (k-q) \big) \Big).$$

since all events have empty intersections, it will be

$$\begin{aligned} P\Big(\big((D_F^I | V \in F) + (D_G^I | V \in F) \big) = k \Big) &= \sum_{q=-\infty}^{+\infty} P\Big(\big((D_F^I | V \in F) = q \big) \cap \big((D_G^I | V \in F) = (k-q) \big) \Big) \\ = \sum_{q=-\infty}^{+\infty} P((D_F^I | V \in F) = q) P((D_G^I | V \in F) = (k-q)) &= [P((D_F^I | V \in F) = q) * P((D_G^I | V \in F) = q)]_k; \end{aligned}$$

the last passages were possible because of the independence of the random variables.

Noting that the random variable represents the degree contribution of the nodes of *F* in a node of *F* seen inside *TM*, $P((D_F^I | V \in F) = q) = f_q^I$ is the degree D_F^I itself. For the variable $(D_G^I | V \in F)$ we observe that a node of *F* has a probability p_{GF} to be connected to a generic node of *G*. Thus, the probability to have *q* links is $p_{GF}^q (1-p_{GF})^{N_G - q}$ multiplied by the number of possible permutations $\binom{N_G}{q}$. We can then express $P((D_G^I | V \in F) = q) = p_{GF}^q (1-p_{GF})^{N_G-q} \binom{N_G}{q} = B_{p_{GF}}^{N_G}(q)$, and we write

$$P(D_{TM}^I = k | V \in F) = [f_q^I * B_{p_{GF}}^{N_G}(q)]_k. \tag{2}$$

With the same method it can be proved that

$$P(D_{TM}^O = k | V \in F) = [f_q^O * B_{p_{FG}}^{N_G}(q)]_k. \tag{3}$$

In the same way for the graph *G*, $P(D_{TM}^I = k | V \in G) = P((D_{TM}^I | V \in G) = k)$. We write the random variable as $(D_{TM}^I | V \in G) = (D_F^I | V \in G) + (D_G^I | V \in G)$, and proceed to also prove that

$$P(D_{TM}^I = k | V \in G) = [g_q^I * B_{p_{FG}}^{N_F}(q)]_k, \tag{4}$$

and

$$P(D_{TM}^O = k | V \in G) = [g_q^O * B_{p_{GF}}^{N_F}(q)]_k. \tag{5}$$

In conclusion, for the indegree, the Eqs. 1, 2 and 4 give

$$P(D_{TM}^I = k) = \frac{N_F}{N_F+N_G} [f_q^I * B_{p_{GF}}^{N_G}(q)]_k + \frac{N_G}{N_F+N_G} [g_q^I * B_{p_{FG}}^{N_F}(q)]_k,$$

and for the outdegree we have

$$P(D^O_{TM} = k) = \frac{N_F}{N_F + N_G}[f^O_q * B^{N_G}_{p_{FG}}(q)]_k + \frac{N_G}{N_F + N_G}[g^O_q * B^{N_F}_{p_{GF}}(q)]_k.$$

If we assume that is always $f^I_k = g^I_k$ and $f^O_k = g^O_k$, and given the bilinearity of convolution, then the indegree becomes

$$P(D^I_{TM} = k) = \left[f^I_q * \left(\frac{N_F}{N_F + N_G}B^{N_G}_{p_{GF}}(q) + \frac{N_G}{N_F + N_G}B^{N_F}_{p_{FG}}(q)\right)\right]_k,$$

and the outdegree becomes

$$P(D^O_{TM} = k) = \left[f^O_q * \left(\frac{N_F}{N_F + N_G}B^{N_G}_{p_{FG}}(q) + \frac{N_G}{N_F + N_G}B^{N_F}_{p_{GF}}(q)\right)\right]_k$$

□

The degree distributions will then be all of the form

$$P(D^I_{TM} = k) = \left[f^I_q * K^I_q\right]_k \tag{6}$$

and

$$P(D^O_{TM} = k) = \left[f^O_q * K^O_q\right]_k. \tag{7}$$

Definition 2. We will call the distributions K^I_q and K^O_q kernels of the convolutions, and f^I_k and f^O_k the starting models. A model with the structure defined above will be defined as convolutional model.

We now prove that this kind of model preserves a power law tail.

Theorem 2. *Consider two probability distributions, f_k e g_k, such that:*

- $\lim_{k\to+\infty} \frac{f_{k-s}}{f_k} = 1, \forall s \geq 0$;
- $\exists l \geq 0 | \forall t > l \Rightarrow g_t = 0$.

If we define $c_k = [f_q * g_q]_k$, then it holds:

$$\lim_{k\to+\infty} \frac{c_k}{f_k} = 1.$$

Proof of Theorem 2. Observe that

$$\frac{c_k}{f_k} = \frac{[f_q * g_q]_k}{f_k} = \frac{\sum_{q=0}^{k} f_q g_{k-q}}{f_k} = \sum_{q=k-l}^{k} \frac{f_q}{f_k} g_{k-q} = \sum_{j=0}^{l} \frac{f_{k-j}}{f_k} g_j$$

since $\lim_{k\to+\infty} \frac{f_{k-j}}{f_k} = 1$ is true by the hypothesis, then

$$\lim_{k\to+\infty} \frac{c_k}{f_k} = \lim_{k\to+\infty} \sum_{j=0}^{l} \frac{f_{k-j}}{f_k} g_j = \sum_{j=0}^{l} \left(\lim_{k\to+\infty} \frac{f_{k-j}}{f_k}\right) g_j = \sum_{j=0}^{l} g_j = 1$$

□

We used these conditions because they are satisfied by f_k, for a power model, and by g_k for a binomial distribution. This result demonstrates that, if we consider models with f_k as a power law and g_k as a finite support, after the convolution we will preserve the asymptotic behavior of f_k. Thus, convolutive models are power law if the starting model is power law and the kernel is finite.

3.2. Random variables

Definition 3. We define $\delta_d(k) = \delta_{dk}$, where d is a non negative integer and δ_{ij} is the Kronecker's delta (1 if the indices are equal and 0 otherwise).

This distribution is the discrete equivalent of the Dirac's delta in the theory of continuum distributions and its fundamental property is equivalent to the continuum case.

Theorem 3. *If f_k is a distribution, then:*

$$[f_q * \delta_d(q)]_k = f_{k-d}.$$

Proof of Theorem 3.

$$[f_q * \delta_d(q)]_k = \sum_{q=-\infty}^{+\infty} f_{k-q}\delta_d(q) = f_{k-d}\delta_d(d) = f_{k-d}$$

□

We note that

$$[f_q * \delta_0(q)]_k = f_k$$

then convolving with δ_0 has no effects on f_k. We now define two random variable that will be used later:

Definition 4. The variable Δ_d is a random variable with distribution $\delta_d(k)$, which represents a random variable with a certain outcome d,

Definition 5. A Bernoulli random variable, that we will denote with X_p, is a random variable with distribution

$$\chi_p(k) = \begin{cases} (1-p), & \text{if } k = 0 \\ p, & \text{if } k = 1 \\ 0, & \text{otherwise} \end{cases}$$

this implements a binary random variable with a probability p to assume the value 1 (for details see [31]).

These random variables have the following properties

- if $Y^1, \ldots, Y^n \sim X_p$, then $\sum_{i=1}^n Y^i = B(n, p)$ which is a binomial random variable;
- $\sum_{i=1}^n \Delta_{d_i} = \Delta_{\sum_{i=1}^n d_i}$;
- for every distribution Z, $Z\Delta_a = aZ$.

3.3. Analysis of the model

To derive the degree distribution of our model, consider a graph F of N_F nodes, with indegree distribution f_k^I and outdegree distribution f_k^O. We initialize the graph B with the disjoint union of two copies of F, which we will call A_1 and A_2. Then $V(B) = V(A_1) \cup V(A_2)$. Because it is a convolutive model, we must obtain

$$P(D_B^I = k) = \left[f_q^I * K_q^I\right]_k$$

for the indegree and, analougously, for the outdegree,

$$P(D_B^O = k) = \left[f_q^O * K_q^O\right]_k,$$

where K_k^I and K_k^O depend only from the connectivity between A_1 and A_2.

Theorem 4. *Defining the graph B as the disjoint union of two copies (A_1 and A_2) of a random model F and subdividing A_1 and A_2 in partions of cardinality l and connecting every partition of A_1 with a partition of A_2 with a connection pattern dependent from the assigned probabilities p, ϕ_U and ϕ_D, it is possible to obtain a graph B such as the degree distributions are:*

$$P(D_B^I = k) = \left[f_q^I * \left(\left((1-p)\delta_0(q) + pB^l_{\phi^U}(q)\right) * \left(p\delta_0(q) + (1-p)B^l_{\phi^D}(q)\right)\right)^{*M}\right]_k \tag{8}$$

and

$$P(D_B^O = k) = \left[f_q^O * \left(\left((1-p)\delta_0(q) + pB^l_{\phi^U}(q)\right) * \left(p\delta_0(q) + (1-p)B^l_{\phi^D}(q)\right)\right)^{*M}\right]_k. \tag{9}$$

Proof of Theorem 4. In order to find K_k^I, we choose a positive integer l, which divides N_F, and we calculate $M = \frac{N_F}{l}$. Then we subdivide A_1 in M random sets of cardinality l, obtaining $A_1^1, \ldots, A_1^M$ partitions of A_1. We proceed in the same way for A_2 obtaining $A_2^1, \ldots, A_2^M$ partitions of A_2. We now define M^2 independent random variables β_{ij} and $\beta'_{ij} \sim X_p$, for $i, j = 1, \ldots, M$, with a fixed $p \in [0, 1]$. They represent connections starting from A_1^i and arriving in A_2^j and from A_2^i and arriving in A_1^j, respectively. Now we define two groups of N_F^2 random variables: $\eta_{st} \sim X_{\phi^U}$ and $\nu_{st} \sim X_{\phi^D}$, for $s \in V(A_1)$ and $t \in V(A_2)$, and where $\phi^U, \phi^D \in [0, 1]$ are two real numbers. In the same way we define $\eta'_{st} \sim X_{\phi^U}$ and $\nu'_{st} \sim X_{\phi^D}$, for $s \in V(A_2)$ and $t \in V(A_1)$.

If the node s in A_1 belongs to A_1^i and the node t in A_2 belongs to A_2^j, the random variable representing the number of edges starting from s and arriving at t is

$$V_{st} = (\eta_{st}\beta_{ij} + \nu_{st}(1 - \beta_{ij})).$$

In the same way,

$$V_{ts} = (\eta'_{ts}\beta'_{ji} + \nu'_{ts}(1 - \beta'_{ji})).$$

Let's calculate $D^I_{A_2}|V(A_1)$; consider a generic $s \in A_1^i$

$$(D^I_{A_2}|V(A_1)) = \sum_{t\in V(A_2)} V_{ts} = \sum_{j=1}^{M}\sum_{w\in A_2^j}(\eta'_{ws}\beta'_{ji} + \nu'_{ws}(1-\beta'_{ji})) = \sum_{j=1}^{M}\left(\beta'_{ji}\sum_{w\in B_j}\eta'_{ws} + (1-\beta'_{ji})\sum_{w\in A_2^j}\nu'_{ws}\right).$$

We observe that if we have a random variable $Z \sim X_\pi$, for some $\pi \in [0, 1]$ and a random variable W with distribution w_k we have, for the probability of the product,

$$P(ZW = k) = \begin{cases} P(Z=0) + P(Z=1)P(W=0) = (1-\pi) + \pi P(W=0), & \text{if } k = 0 \\ P(Z=1)P(W=k) = \pi P(W=k), & \text{else} \end{cases}$$

so we can write $P(WZ = k) = (1-\pi)\delta_0(k) + \pi w_k$. Under this condition, it will be

$$P((D^I_{A_2}|V \in V(A_1)) = k) = \left[\left((1-p)\delta_0(q) + pB^I_{\phi^U}(q)\right) * \left(p\delta_0(q) + (1-p)B^I_{\phi^D}(q)\right)\right]^{*M}_k,$$

where $^*M$ at exponent is the M-th power convolution. With an analogous procedure we obtain

$$K^I_k = K^O_k = P((D^O_{A_2}|V \in V(A_1)) = k) = P((D^I_{A_1}|V \in V(A_2)) = k) = P((D^O_{A_1}|V \in V(A_2)) = k) =$$

$$= \left[\left((1-p)\delta_0(q) + pB^I_{\phi^U}(q)\right) * \left(p\delta_0(q) + (1-p)B^I_{\phi^D}(q)\right)\right]^{*M}_k.$$

Finally, we have

$$P(D^I_B = k) = \left[f^I_q * \left(\left((1-p)\delta_0(q) + pB^I_{\phi^U}(q)\right) * \left(p\delta_0(q) + (1-p)B^I_{\phi^D}(q)\right)\right)^{*M}\right]_k \tag{10}$$

and

$$P(D^O_B = k) = \left[f^O_q * \left(\left((1-p)\delta_0(q) + pB^I_{\phi^U}(q)\right) * \left(p\delta_0(q) + (1-p)B^I_{\phi^D}(q)\right)\right)^{*M}\right]_k \quad \square \tag{11}$$

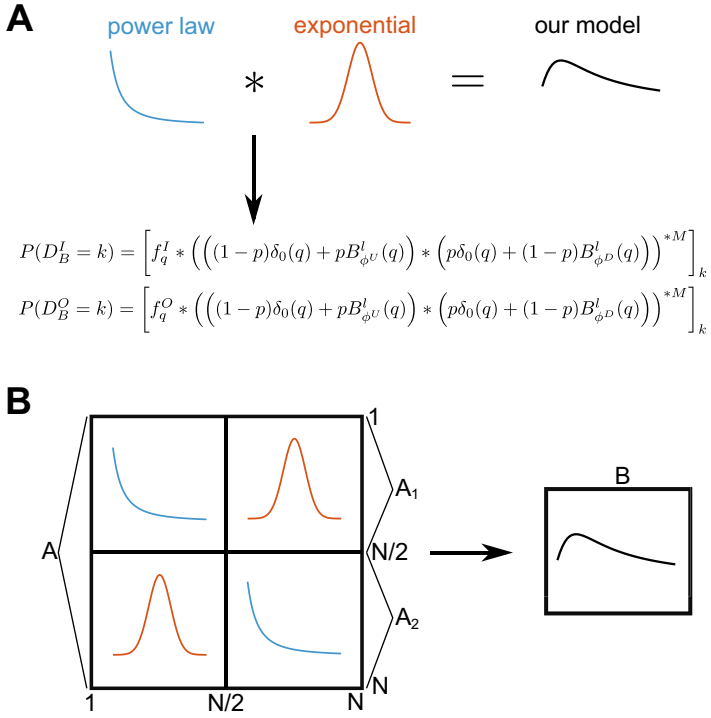

Fig. 2. Schematic representation of the model. A) (top) schematic representation of the convolution process; (bottom) the equations describing the result of the convolution between the two original models to obtain the in- and out-degrees of the new model (see Suppl. Material for their derivation). B) Graphical illustration of the convolution process, which starts from the connectivity matrix of a network B and its blocks A_1 and A_2. The final connectivity matrix B is calculated by considering the two power law blocks on the main diagonal and two exponential blocks in the antidiagonal of B as indicated in the diagram. Each subblock is a $\frac{N}{2} \times \frac{N}{2}$ matrix.

These are the equations to use to analyze and reproduce a network with the same connectivity observed in brain networks. Of course they can also be used to create new networks with the desired connectivity properties. The procedure is synthetically depicted in Fig. 2.

3.4. Implementation of the model

We will generate a graph B from A_1 and A_2, where the graph A_1 and A_2 are BA model graphs with initial configuration a ER graph with m_0 nodes and probability ρ with N nodes and Σ, a, l, p, ϕ^U and ϕ^D are other parameters. A pseudocode to generate the graph B is shown in Figure Algorithm 1.

Algorithm 1 Generate a new graph from two BA model graphs.

```
function GraphGen(Σ, a, m_0, ρ, l, N, p, φ_U, φ_D)
    A_1 = BA(Σ, a, m_0, ρ)
    A_2 = BA(Σ, a, m_0, ρ)
    B = A_1 ∪ A_2
    M = N/l
    create {A_1^1, ..., A_1^M} partition of A_1
    create {A_2^1, ..., A_2^M} partition of A_2
    for i ∈ {1, ..., M} do
        for j ∈ {1, ..., M} do
            r_1 = random number between [0,1] with uniform distribution
            if r_1 < p then
                s_1 = random number between [0,1] with uniform distribution
                if s_1 < φ_U then
                    Add an edge from every node of A_1^i to every node of A_2^j inside B
                end if
            else
                s_1 = random number between [0,1] with uniform distribution
                if s_1 < φ_D then
                    Add an edge from every node of A_1^i to every node of A_2^j inside B
                end if
            end if
            r_2 = random number between [0,1] with uniform distribution
            if r_2 < p then
                s_2 = random number between [0,1] with uniform distribution
                if s_2 < φ_U then
                    Add an edge from every node of A_2^j to every node of A_1^i inside B
                end if
            else
                s_2 = random number between [0,1] with uniform distribution
                if s_2 < φ_D then
                    Add an edge from every node of A_2^j to every node of A_1^i inside B
                end if
            end if
        end for
    end for
end function
```

3.5. Convolutive equations

Suppose that f_k and h_k are two probability distributions (zero for negative k). We would like to know if exist a succession g_k (zero for negative k) such as

$$[f_q * g_q]_k = h_k, \forall k \geq 0$$

and if this g_k, which is the solution of a convolutional equation, is unique. As a starting point we will suppose a weak equation, i.e.

$$[f_q * g_q]_k = h_k, 0 \leq k \leq k_s$$

where k_s is a positive integer.

Theorem 5. *If $f_0 \neq 0$ then the solution of the equation exists and it is unique:*

$$[f_q * g_q]_k = h_k, 0 \leq k \leq k_s,$$

for any positive integer k_s.

Proof of Theorem 5. Rearranging this equation we observe that is equivalent to the linear system

$$\begin{cases} f_0 g_0 = h_0 \\ f_1 g_0 + f_0 g_1 = h_1 \\ \dots \\ f_{k_s} g_0 + \dots + f_0 g_{k_s} = h_{k_s} \end{cases} \tag{12}$$

and we observe that if $f_0 \neq 0$ then the system is Kramerian and it admits only one solution. Also the infinite equation have only one solution, because if we suppose two distinct solutions then they must differ in at least one k; let it $\bar{k}$ the minimum k for which it happens, then the problem

$$[f_q * g_q]_k = h_k, 0 \leq k \leq \bar{k}$$

has two distinct solutions, which is a contradiction □

Following this result we write the deconvolution as

$$g_k = [h_q *^{-1} f_q]_k$$

meaning that g_k is the only solution of the equation

$$[f_q * g_q]_k = h_k.$$

Theorem 6. *The equation $[g_q * \delta_d(q)]_k = h_k$ (with $d > 0$) has solution if only if $h_0 = \dots = h_{d-1} = 0$.*

Proof of Theorem 6. The deconvolution system takes the form

$$\begin{cases} 0 = \delta_d(0) g_0 = h_0 \\ \dots \\ 0 = h_{d-1} \\ g_0 = h_d \\ \dots \\ g_{k-d} = h_k \end{cases}$$

and we observe that it has a solution only if $h_0 = \dots = h_{d-1} = 0$ □

This trivial result derives from the fact that $\delta_d(0) = 0$, negating the condition guaranteeing that the deconvolution exists and is unique. The other equations suggest that $g_k = h_{k+d}$. We observe that if h_k is positive for $k < d$ this equations doesn't admit any solution.

If we assume that $g_k = h_{k+d}$ is an approximate solution, it will be:

$$[g_q * \delta_d(q)]_k = \sum_{q=-\infty}^{+\infty} g_{k-q} \delta_d(q) = \sum_{q=-\infty}^{+\infty} h_{k-q+d} \delta_d(q) = \begin{cases} 0, & \text{if } 0 \leq k \leq d-1 \\ h_k, & \text{if } k > d-1 \end{cases}$$

we observe that we have lost the values of h_k before d. In other words, by ignoring the first d equations we have lost information. We suppose now to fix a $\varepsilon \in]0, 1[$ and, in order to obtain a convex linear combination, we try to solve the new equation

$$[g_q * (\varepsilon \delta_0(q) + (1-\varepsilon)\delta_d(q))]_k = h_k \tag{13}$$

this equation is a perturbation of the previous one, and it respects the hypothesis that $\varepsilon \delta_0(0) + (1-\varepsilon)\delta_d(0) = \varepsilon \neq 0$. Then a solution exists and is unique for every h_k. In particular, calling the solution g_k^ε, following Eqs. 13 and 12, we have

$$g_k^\varepsilon = [h_q *^{-1} (\varepsilon \delta_0(q) + (1-\varepsilon)\delta_d(q))]_k = \begin{cases} \frac{h_k}{\varepsilon}, & \text{if } 0 \leq k \leq d-1 \\ \frac{h_k}{\varepsilon} - \frac{(1-\varepsilon)h_{k-d}}{\varepsilon^2}, & \text{if } k > d-1 \end{cases}$$

and we observe that for $\varepsilon \to 0$ then g_k^ε goes to infinity. This example explain how a little perturbations of the kernel can lead to large changes in the deconvolution.

3.6. Fitting a distribution

To calculate the degrees of the new graph, we start by declaring m_0, ρ and l as independent parameters; we also introduce a shape parameter of the model, E_K.

Theorem 7. *By fixing the parameters m_0, ρ and l and a shape parameter E_K, it is possible to find a combination of parameters of the model such as*

$$P(D_B^l = k) \approx v_k^l.$$

Proof of Theorem 7. The idea is to approximate the indegree equation (see Eqs. 6 and 7)

$$\left[\left(\frac{N - m_0}{N} \sigma_q + \frac{m_0}{N} B_\rho^{m_0 - 1}(q) \right) * K_q^l \right]_k = v_k^l,$$

with an equation of this form

$$\left[\left(\frac{N-m_0}{N}\sigma_q + \frac{m_0}{N}B_\rho^{m_0-1}(q)\right) * \delta_d(q)\right]_k = v_k^I.$$

The problem is to find the parameters σ_k, d, a and p. In order to find d, we first rewrite the equation in the form

$$[\alpha_q * \delta_d(q)]_k = v_k^I,$$

and we impose that $\mathbb{E}(\alpha_k) = \mathbb{E}(v_k^I) - E_K = E_V - E_K$, because $\mathbb{E}(\left[\alpha_q * K_q^I\right])_k = \mathbb{E}(\alpha_k) + \mathbb{E}(K_k^I) = E_V - E_K + E_K = E_V = \mathbb{E}(v_k^I)$.

We also note that, since the equation

$$[\alpha_q * \delta_d(q)]_k = v_k^I,$$

can not be solved under certain conditions (see previous subsection), we will define α_k as an approximation of a solution.

Note that $\alpha_k = \frac{v_{k+d}^I}{\sum_{s=d}^{+\infty} v_s^I}$ is a distribution. Then we can calculate the expected value as follows

$$\begin{aligned}\mathbb{E}(\alpha_k) &= \sum_{k=0}^{+\infty} k\alpha_k = \sum_{k=0}^{+\infty} k\frac{v_{k+d}^I}{\sum_{s=d}^{+\infty} v_s^I} = \frac{\sum_{k=0}^{+\infty} k v_{k+d}^I}{\sum_{s=d}^{+\infty} v_s^I} = \frac{\sum_{s=d}^{+\infty}(s-d)v_s^I}{\sum_{s=d}^{+\infty} v_s^I} = \frac{\sum_{s=d}^{+\infty} s v_s^I - d\sum_{s=d}^{+\infty} v_s^I}{\sum_{s=d}^{+\infty} v_s^I} \\ &= \frac{E_V - \sum_{j=0}^{d-1} j v_j^I - d\left(1-\sum_{j=0}^{d-1} v_j^I\right)}{1-\sum_{j=0}^{d-1} v_j^I}.\end{aligned}$$

Remembering that α_k is still dependent from d, which is a free variable, we can impose the condition on the expected value creating the system

$$\begin{cases}\mathbb{E}(\alpha_k) = \dfrac{E_V - \sum_{j=0}^{d-1} j v_j^I - d\left(1-\sum_{j=0}^{d-1} v_j^I\right)}{1-\sum_{j=0}^{d-1} v_j^I} = \varphi\left(d, v_k^I\right) \\ \mathbb{E}(\alpha_k) = E_V - E_K.\end{cases}$$

From the above system, defining $\hat{k}$ as the biggest integer such as $v_{\hat{k}}^I > 0$, we find

$$d = \arg\min_{d\in\{0,\dots,\hat{k}\}} |(E_V - E_K) - \varphi(d, v_k^I)|.$$

From d we also find α_k, as

$$\alpha_k = \frac{N-m_0}{N}\sigma_k + \frac{m_0}{N}B_\rho^{m_0-1}(k)$$

and then we have

$$\sigma_k = \frac{N}{N-m_0}\alpha_k - \frac{m_0}{N-m_0}B_\rho^{m_0-1}(k).$$

From this equation it also follows that $a = \mathbb{E}(\Sigma) = \frac{N}{N-m_0}(E_V - E_K) - \frac{m_0}{N-m_0}\rho(m_0-1)$. The reason why $a = \mathbb{E}(\Sigma)$ lays in the fact that the decay has exponent $2 + \frac{a}{\mathbb{E}(\Sigma)}$.

In order to find p, we observe that

$$\begin{aligned}E_K &= \mathbb{E}\left(\left[\left(\left((1-p)\delta_0(q) + pB_{\phi^U}^I(q)\right) * \left(p\delta_0(q) + (1-p)B_{\phi^D}^I(q)\right)\right)^{*M}\right]_k\right) \\ &= M\,\mathbb{E}\left(\left[\left((1-p)\delta_0(q) + pB_{\phi^U}^I(q)\right) * \left(p\delta_0(q) + (1-p)B_{\phi^D}^I(q)\right)\right]_k\right) \\ &= M\left(\mathbb{E}\left(\left[\left((1-p)\delta_0(q) + pB_{\phi^U}^I(q)\right)\right]_k\right) + \mathbb{E}\left(\left[\left(p\delta_0(q) + (1-p)B_{\phi^D}^I(q)\right)\right]_k\right)\right) \\ &= M(pI\phi_U + (1-p)I\phi_D) = N(p\phi_U + (1-p)\phi_D).\end{aligned}$$

Then we have the linear equation

$$E_K = N(p\phi_U + (1-p)\phi_D)$$

which solved in p returns $p = \frac{\frac{E_K}{N} - \phi^D}{\phi^U - \phi^D} \approx \frac{E_K}{N}$ (for $\phi^U \approx 1$ and $\phi^D \approx 0$).

In conclusion, substituting in Eqs. 8 and 9 the values $f_k^I = \alpha_k$ and $f_k^O = \frac{B\left(k+a, 2+\frac{a}{c}\right)}{B\left(a, 1+\frac{a}{c}\right)}$, we have

$$P(D_B^I = k) = \left[\alpha_k * \left(\left((1-p)\delta_0(q) + pB_{\phi^U}^I(q)\right) * \left(p\delta_0(q) + (1-p)B_{\phi^D}^I(q)\right)\right)^{*M}\right]_k \approx v_k^I$$

and

$$P(D_B^O = k) = \left[\frac{B\left(k+a, 2+\frac{a}{c}\right)}{B\left(a, 1+\frac{a}{c}\right)} * \left(\left((1-p)\delta_0(q) + pB_{\phi^U}^I(q)\right) * \left(p\delta_0(q) + (1-p)B_{\phi^D}^I(q)\right)\right)^{*M}\right]_k$$

□

4. Results and discussion

We tested our model with two quite different sets of data on cell-to-cell connectivity, to validate the results under two extreme conditions: three network instances of a large-scale, highly validated and biologically realistic, neocortical column model [33], downloaded from the neocortical portal (https://bbp.epfl.ch/nmc-portal/downloads), and seven small (approximately 100 neurons) subnetworks of GABAergic hippocampal neurons, recorded in vitro from different slices [32].

For the neocortical column model, we separately analyzed the relatively large excitatory and inhibitory networks (composed by approximately 26,000 and 5,000 neurons, respectively); the probability distributions (see Fig. 3A) show a low variability among the different network instances. They follow the general shape expected for a brain network, with no disconnected neurons, a decreasing number of highly connected neurons, and no fully connected neurons. A direct comparison of the survival function for these networks with that obtained from a pure exponential or a power law model (see black and orange lines in Fig. 3B), demonstrates the peculiar properties of brain networks' connectivity, and illustrates why it has been impossible to describe it by a theoretical model so far. In striking contrast with the neocortical column networks, the survival function for the in- and out-degrees calculated from the hippocampal slices, exhibited a rather large variability (Fig. 3C). This is somewhat expected, since just a few hundred neurons belonging to a much larger network were sampled (there are many thousands of GABAergic neurons in a rat hippocampus). Very interestingly, a network of a similar number of neurons but composing the entire nervous system of a C. elegans (Fig. 3C dotted line) shows a relatively similar connectivity. A deeper look at the shape of these plots also reveals the possible consequence of the slicing process. By cutting many existing connections, this procedure can artificially increase the observed number of poorly connected neurons. The effect can be inferred by the large negative values of the survival function for low degrees, which is more evident for incoming connections (see orange and dark blue plots in Fig. 3C). This is clearer in the typical distributions shown in Fig. 3D for two typical slices, in which the lowest degree has the highest probability to occur.

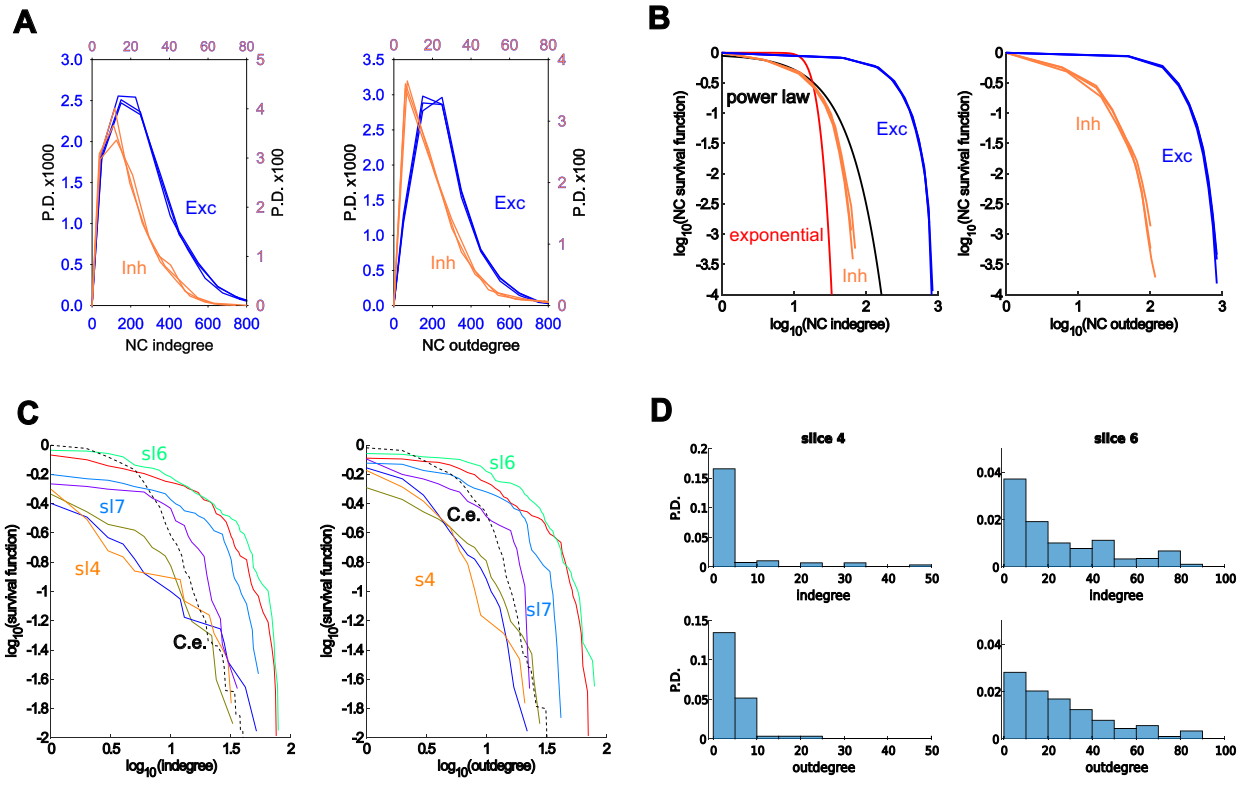

Fig. 3. in- and out-degree from brain networks. A) Probability density of in- and out-degree for the excitatory (blue plots) and inhibitory (orange plots) neurons in three instances of the NC model network. Raw data were downloaded from (https://bbp.epfl.ch/nmc-portal/downloads) B) survival functions calculated from the plots in A); for comparison, the lines representing a power law (with degree distribution $f_k = \frac{B(a+k,2+\frac{a}{c})}{B(a,1+\frac{a}{c})}$ with $c = 17$ and $a = 100c$) and an exponential (with degree distribution $g_k = \binom{N-1}{k} p^k (1-p)^{N-1-k}$ with $p = .0033$ and $N = 5180$) model are also shown. C) survival functions calculated from the data obtained in vitro in 7 slices (different line color) from neurons in the GABAergic CA3 region (from [32]). For comparison, the survival function obtained from the C. elegans network composed by all neurons connected through chemical synapses is also plotted (C.e., black dotted line, data taken and redrawn from [30]); the function for three slices are (sl4, sl6, and sl6) are explicitly indicated D) The in- and out-degree distribution for slice 4 and 6. (For interpretation of the references to colour in this figure legend, the reader is referred to the web version of this article.)

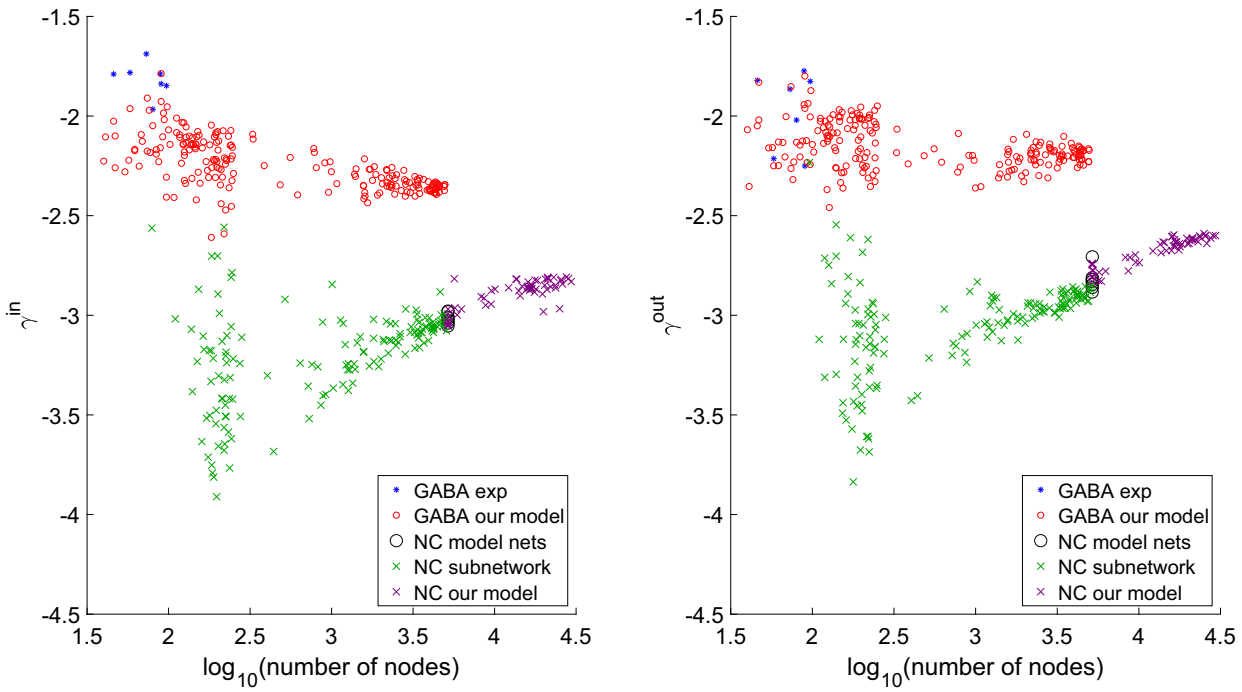

Fig. 4. Large-scale network connectivity can be extrapolated by sampling a set of subnetworks. (Left) γ for the indegree distribution as a function of network size, in terms of number of nodes (log10 scale); Blue symbols represent the γ values calculated from the experimental data recorded from CA1 interneurons in 7 hippocampal slices; Red symbols represent the γ values for networks composed by different number of nodes, obtained by randomly sampling a 5,000-neurons network built with our model using parameters that best fit the experimental distributions. Black symbols are the γ values calculated from 7 instances of the approximately 5000 neurons composing the NC inhibitory network. Green symbols represent the γ values obtained from smaller networks, randomly sampled from the 5,000-neuron network from [33]. Purple symbols represent our models projection for larger networks. (Right) same as in the left panel but for outdegrees.

Taken together, these results suggest that there might be a lower limit to the number of neurons that should be investigated to effectively characterize the network to which they belong, and also point to the need of finding a method to extrapolate the full network behavior from a sparse set of data. To better illustrate the results that can be obtained with our model, and to make an easier comparison with the analyses carried out in the field so far, we used the γ value best fitting the tail of the distributions as a reference parameter. Let's first consider the relatively large inhibitory network of the neocortical column model. From the 7 network instances downloaded from (https://bbp.epfl.ch/nmc-portal/downloads) we calculated the γ for the in- and out-degree distributions (black symbols in Fig. 4). We then sampled, from the original network, many other smaller networks by changing only the number of neurons (green symbols in Fig. 4).

In other words, we made a series of in silico experiments, in which we sampled subnetworks of different size composed by neurons randomly chosen from the 5,000-neuron network. Instead, to extrapolate the results to a larger network, we fitted one of the 5000-neuron networks with our model and used the same parameters to build a 30,000-neuron network by just upscaling the degree distributions by a factor of. Again, we then made a series of in silico experiments, in which we sampled subnetworks of different size composed by neurons randomly chosen from the full 30,000-neuron network. These networks had γ values that approached those obtained from the 7 original networks (purple symbols in Fig. 4). However, the γ values systematically decreased for smaller and smaller subnetworks, with a sudden more dramatic spread of values for networks composed by only a few hundred neurons. These results indicate that the connectivity properties of a network may not be properly assessed by subsampling, because the resulting connectivity can be quite different. One way to resolve this problem is to always sample a number of neurons more representative of the full network size.

Unfortunately, this is not always technically possible, and a much lower number can be usually tested, as for the hippocampal gabaergic network in this work. To find out whether we could extrapolate the full network properties from these data, we calculated the γ from the seven slices (blue symbols in Fig. 4) by fitting each of them with our model. The average value was then used to build a network of 5000 neurons. We hypothesized that if this large network (roughly one-third of the real hippocampal CA3 GABAergic network) was a plausible representation of the real network, in silico experiments sampling smaller subnetworks should end up with values of γ consistent with those found experimentally for the seven slices. The results (red symbols in Fig. 4) confirmed our hypothesis: the cloud of γ values obtained for the outdegrees of networks composed by a few hundred neurons were consistent with those found experimentally (Fig. 4, right, compares blue and red symbols). Those obtained for the indegree (Fig. 4, left plot) showed some discrepancy, with

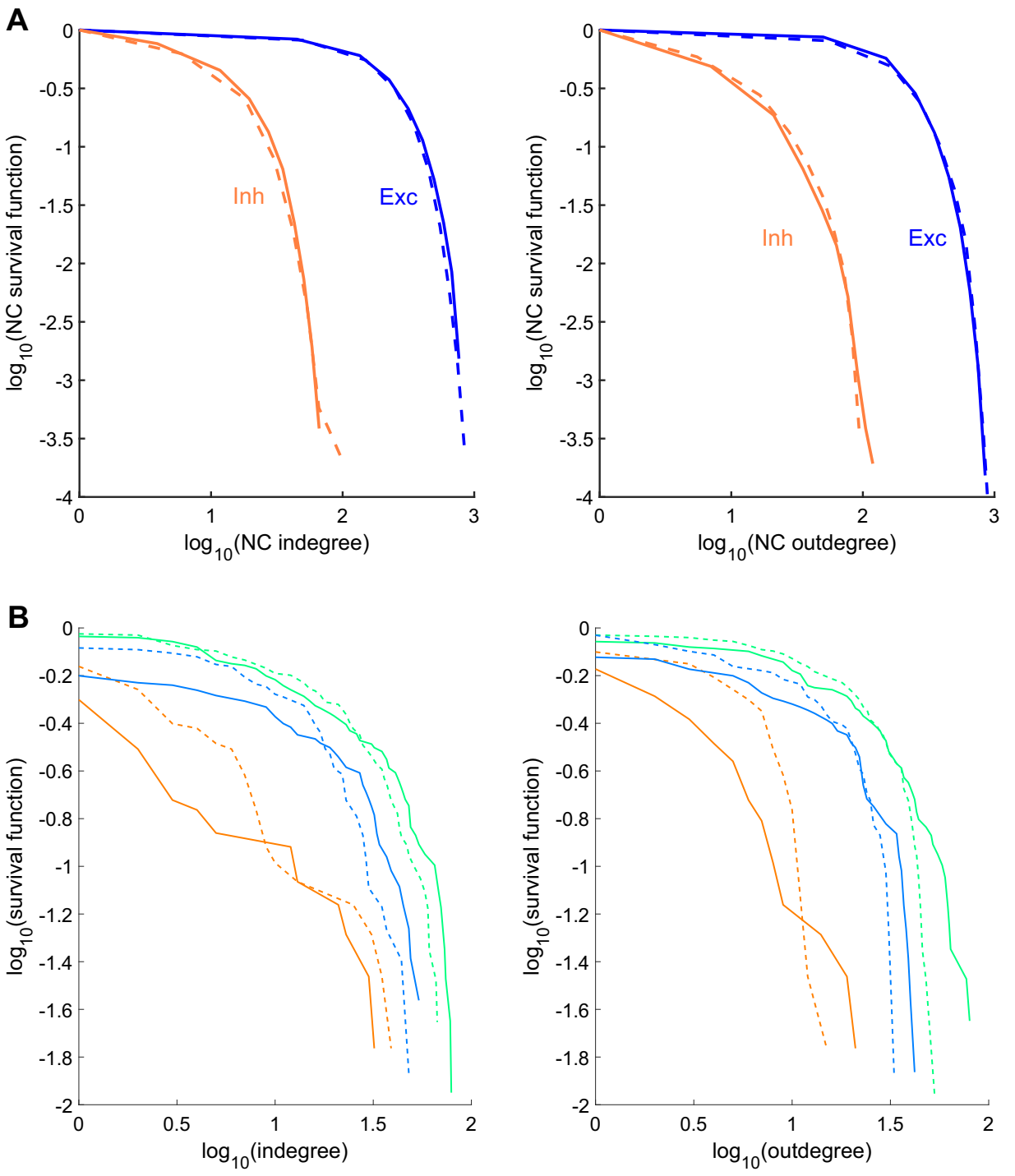

Fig. 5. The new approach results in a quantitative agreement between model and data. A) Comparison between the survival functions of one of the NC datasets (solid lines) and our model (dotted lines) ($p < .025$ for both the populations, with the Exc-Inh and Inh-Exc terms calculated from Kolmogorov-Smirnov distance). B) three representative experimental slices (solid lines) and three similar networks (dotted lines) extracted from the 5000 nodes network generated with our algorithm ($p < .1$ for orange, blue, and green traces calculated comparing γ distributions of best fits). (For interpretation of the references to colour in this figure legend, the reader is referred to the web version of this article.)

the experimental findings exhibiting less connectivity (i.e. higher γ). This result suggests a bias in the number of observed incoming connections caused by the slicing process.

Furthermore, it suggests that to fully and correctly characterize a network's connectivity, it can be sufficient to analyze (with our model) several instances of a relatively smaller network, and then extrapolate these to a network size more representative of the real system. This approach should be applied whenever the real network size is much larger than the measured sample. Very large networks, such as an entire brain region, may not be sufficiently described by sampling only once even thousands of neurons. This is suggested by the gamma values obtained for inhibitory cortical networks larger than 5000 neurons (cyan symbols in Fig. 4). In this case, the values keep increasing with the network size, in striking contrast with the hippocampal slices, which are relatively constant for networks larger than several hundreds of neurons. This suggests that the cortical column model may not represent the full connectivity properties of the corresponding entire cortical region.

A more detailed comparison between data and model is shown in Fig. 5, here our model can quantitatively reproduce all in- and out-degree cumulative distributions for both the neocortical column model (Fig. 5A) and the experimental findings from hippocampal slices (Fig. 5B). The results for the hippocampal slices are particularly interesting because they show how the model can quantitatively capture the physiological variability observed experimentally by sparsely sampling a much bigger network. It is important to note that the distributions best reproducing the experimental data (Fig. 5B, dotted lines) were just found by sampling, from the full network, subnetworks with the same number of neurons recorded in the experiments. Although (by considering the γ distributions of the best fits) they are all statistically indistinguishable from their experimental counterpart, it should be stressed that these networks do not have the slicing effect observed for the indegrees. This can be explained by the fact that they were sampled from an intact network. In other words, the model is able to predict the real distribution that may be expected for a small subnetwork.

5. Conclusions

Several fundamental conclusions can be drawn from this work. First of all, it introduces a mathematical framework to quantitatively reproduce the entire range of a brain network's connectivity, a vital step to better understand information processing in the brain. Also, the proposed model is the only way available so far to extract the full network connectivity from a few sets of experimental recordings of small subnetworks, and it is able to provide an indication on whether experimentally tested subnetworks are a reasonable representation of the full system's connectivity. Furthermore, the model changes the paradigm with which large-scale model networks can be built, from probabilistic/empiric connections or limited (and most likely also misleading) data, to a process based on a rigorous theoretical background that can algorithmically generate networks composed by neurons connected as in the real systems. This is important because, as previously noted [34], the degrees distribution is the only information necessary to fully characterize the general properties of a large network. Finally, this new theoretical framework gives the intriguing possibility to investigate in more details both functional and dysfunctional network connectivity properties. This aspect can have a paramount role in finding innovative methods or indicators to identify the most influential nodes within a network [35], opening the way to design innovative molecular targets. From a more general point of view, the same framework described here for brain networks can also be applied to social networks [36] and real-world complex networks [37,38].

6. Authors contributions

G Giacopelli created and implemented the model and performed all analyses; D Tegolo conceived the study and contributed to the creation and implementation of the model; M Migliore conceived the study and wrote the manuscript, with contributions from all authors.

7. Data and materials availability

All data used in this paper and the code implementing the model are available for public download in the live papers section of the Human Brain Project Brain Simulation Platform https://humanbrainproject.github.io/hbp-bsp-live-papers/2020/giacopelli_et_al_2020/giacopelli_et_al_2020.html, and on ModelDB (https://senselab.med.yale.edu/modeldb/enterCode?model=261881).

Acknowledgment

We thank Rosa Cossart and Paolo Bonifazi for kindly providing the raw data on the hippocampal neurons. Editorial support, in an early version of the manuscript, was provided by Annemieke Michels of the Human Brain Project.

References

[1] Y. Zhang, P. Xu, K. Cheng, D. Yao, Multivariate synchronization index for frequency recognition of ssvep-based brain-computer interface, J. Neurosci. Methods 221 (2014) 32–40.
[2] P. Uhlhaas, W. Singer, Abnormal neural oscillations and synchrony in schizophrenia, Nat. Rev. Neurosci. 11 (2) (2010) 100–113.

[3] C. Stam, J. Reijneveld, Graph theoretical analysis of complex networks in the brain, Nonlinear Biomed Phys 1 (2007).
[4] M. Ahmadlou, H. Adeli, Functional community analysis of brain: a new approach for eeg-based investigation of the brain pathology, Neuroimage 58 (2) (2011) 401–408.
[5] A. Fornito, A. Zalesky, M. Breakspear, The connectomics of brain disorders, Nat. Rev. Neurosci. 16 (3) (2015) 159–172.
[6] J. Hindmarsh, R. Rose, A model of neuronal bursting using three coupled first order differential equations, Proceedings of the Royal Society of London. Series B, Containing papers of a Biological character. Royal Society (Great Britain) 221 (1222) (1984) 87–102.
[7] E. Spera, M. Migliore, N. Unsworth, D. Tegolo, On the cellular mechanisms underlying working memory capacity in humans, Neural Network World 26 (4) (2016) 335–350.
[8] Y. Shang, Mixed si (r) epidemic dynamics in random graphs with general degree distributions, Appl Math Comput 219 (10) (2013) 5042–5048.
[9] J. Aledo, L. Diaz, S. Martinez, J. Valverde, Dynamical attraction in parallel network models, Appl Math Comput 361 (2019) 874–888.
[10] M. Oğuztöreli, G. Steil, T. Caelli, Control mechanisms of a neural network, Biol Cybern 54 (1) (1986) 21–28.
[11] A. Omurtag, B. Knight, L. Sirovich, On the simulation of large populations of neurons, J Comput Neurosci 8 (1) (2000) 51–63.
[12] B. Knight, A. Omurtag, L. Sirovich, The approach of a neuron population firing rate to a new equilibrium: an exact theoretical result, Neural Comput 12 (5) (2000) 1045–1055.
[13] M. Rigby, M. Anthonisen, X. Chua, A. Kaplan, A. Fournier, P. Grütter, Building an artificial neural network with neurons, AIP Adv 9 (7) (2019).
[14] Z. Cheng, J. Cao, Synchronization of a growing chaotic network model, Appl Math Comput 218 (5) (2011) 2122–2127.
[15] S. Herculano-Houzel, R. Lent, Isotropic fractionator: a simple, rapid method for the quantification of total cell and neuron numbers in the brain, J. Neurosci. 25 (10) (2005) 2518–2521.
[16] S. Jbabdi, S. Sotiropoulos, S. Haber, D. Van Essen, T. E Behrens, Measuring macroscopic brain connections in vivo, Nat. Neurosci. 18 (2015) 1546–1555.
[17] T.B. Dyrby, L.V. Søgaard, G.J.M. Parker, D.C. Alexander, N.M. Lind, W.F.C. Baaré, A. Hay-Schmidt, N. Eriksen, B. Pakkenberg, O.B. Paulson, J. Jelsing, Validation of in vitro probabilistic tractography, Neuroimage 37 (2007) 1267–1277.
[18] J.W. Lichtman, W. Denk, The big and the small: challenges of imaging the brain's circuits., Science 334 6056 (2011) 618–623.
[19] I.R. Wickersham, E.H. Feinberg, New technologies for imaging synaptic partners, Curr. Opin. Neurobiol. 22 (2012) 121–127.
[20] P. Erdos, A. Renyi, On the evolution of random graphs, Publ. Math. Inst. Hungary. Acad. Sci. 5 (1960) 17–61.
[21] M.J. Newman, Networks: An introduction, 2010.
[22] A.-L. Barabási, R. Albert, Emergence of scaling in random networks, Science 286 (5439) (1999) 509–512.
[23] F. W. Olver, D. Lozier, R. Boisvert, C. Clark, Nist handbook of mathematical functions(2010).
[24] G. Gong, Y.R. He, L. Concha, C.A. Lebel, D.W. Gross, A.C. Evans, C. Beaulieu, Mapping anatomical connectivity patterns of human cerebral cortex using in vivo diffusion tensor imaging tractography., Cerebral cortex 19 3 (2009) 524–536.
[25] P. Hagmann, L. Cammoun, X. Gigandet, R.A. Meuli, C.J. Honey, V.J. Wedeen, O. Sporns, Mapping the structural core of human cerebral cortex, PLoS Biol. 6 (2008) 245–251.
[26] M.P. Van den Heuvel, O. Sporns, Rich-club organization of the human connectome., J. Neurosci. 31 44 (2011) 15775–15786.
[27] M.T. Stobb, J.M. Peterson, B. Mazzag, E. Gahtan, Graph theoretical model of a sensorimotor connectome in zebrafish, PloS one, 2012.
[28] D.S. Modha, R.P. Singh, Network architecture of the long-distance pathways in the macaque brain., Proc. Natl. Acad. Sci. U.S.A. 107 30 (2010) 13485–13490.
[29] M.P. Van den Heuvel, O. Sporns, Network hubs in the human brain, Trends Cogn. Sci. (Regul. Ed.) 17 (2013) 683–696.
[30] L.R. Varshney, B.L. Chen, E. Paniagua, D.H. Hall, D.B. Chklovskii, Structural properties of the caenorhabditis elegans neuronal network, PLoS Computational Biology, 2009.
[31] M. Evans, N. Hastings, B. Peacock, Statistical distributions, Wiley Series in Probability and Statistics, Wiley, 2000.
[32] P. Bonifazi, M. Goldin, M.A. Picardo, I. Jorquera, A. Cattani, G. Bianconi, A. Represa, Y. Ben-Ari, R. Cossart, Gabaergic hub neurons orchestrate synchrony in developing hippocampal networks., Science 326 5958 (1970) 1419–1424.
[33] H. Markram et Al., Reconstruction and simulation of neocortical microcircuitry, Cell 163 (2) (2015) 456–492.
[34] D.Q. Nykamp, D. Friedman, S.M. Shaker, M. Shinn, M. Vella, A. Compte, A. Roxin, Mean-field equations for neuronal networks with arbitrary degree distributions., Physical review. E 95 4-1 (2017) 042323.
[35] G. Sabidussi, The centrality index of a graph, Psychometrika 31 (4) (1966) 581–603.
[36] L.C. Freeman, Centrality in social networks conceptual clarification, Soc Networks 1 (3) (1978) 215–239.
[37] J. Wang, C. Li, C. Xia, Improved centrality indicators to characterize the nodal spreading capability in complex networks, Appl Math Comput 334 (C) (2018) 388–400.
[38] C. Li, L. Wang, S. Sun, C. Xia, Identification of influential spreaders based on classified neighbors in real-world complex networks, Appl Math Comput 320 (2018) 512–523.
[39] F. Cavarretta, D.T. Carnevale, D. Tegolo, M. Migliore, Effects of low frequency electric fields on synaptic integration in hippocampal ca1 pyramidal neurons: implications for power line emissions, Frontiers in Cellular Neuroscience 8 (2014) 310.